Kinetic electron excitation in the interaction of slow Kr$^+$ ions with Al surfaces

M. Commisso,[1] M. Minniti,[1] A. Sindona,[1] A. Bonanno,[1] A. Oliva,[1] R. A. Baragiola,[2] and P. Riccardi[1,*]

[1]*Laboratorio IIS, Università della Calabria and INFN—gruppo collegato di Cosenza—87036 Rende, Cosenza, Italy*
[2]*Laboratory for Atomic and Surface Physics, University of Virginia, Engineering Physics, Charlottesville, Virginia 22904, USA*

We report experimental studies of electron emission in the interaction of 1–8 keV Kr$^+$ ions with clean Al surfaces. We observe that total electron emission yield depends exponentially on v^{-1}, the inverse of the velocity of the projectiles, rather than on the inverse of the component of v orthogonal to the surface, expected in the recently proposed surface-assisted kinetic electron emission. The energy distributions of emitted electrons show well-known features of kinetic electron emission: a broad continuum background with superimposed structures due to the decay of bulk plasmons and to Auger decay of Al-2p excitations produced by electron promotion. The close correlation of the intensities of electron emission from Auger and plasmon decay with the total electron yields leads to the conclusion that kinetic electron emission in Kr$^+$ interactions with Al surfaces is dominated by electron promotion in close atomic collisions.

I. INTRODUCTION

The spectroscopy of electrons emitted in slow ion-surface interactions gives valuable information on fundamental excitation processes resulting from ion impact. Most of the studies of electron excitation and emission have been performed using metal samples and, although the phenomenon has been studied for decades,[1] substantial developments and basic mechanisms are still being discovered or proposed.[2–4]

Ion induced electron emission from solids is due to the main types of processes: potential and kinetic electron emission.[1] In potential electron emission (PEE), electron excitation occurs when the potential energy carried by the incident ion is released upon neutralization by electron capture from the surface. In kinetic electron emission (KEE), excitation results from the transfer of the kinetic energy of incoming particles.

Basic mechanisms of KEE from metal surfaces are excitations of solid valence electrons in binary projectile-electron collisions in an idealized Fermi electron gas,[5] and electron promotion in close atomic collisions.[6] Both these processes are subject to a threshold impact velocity or energy below which no electron emission should be possible. Electron promotion, important for heavier projectiles, occurs at or below the surface, when close collisions temporarily create quasi-molecules in which some electronic levels are promoted to higher orbital energies, giving rise to direct electron emission or delayed emission after Auger de-excitation[1,7,8] or after autoionization of excited states formed by electron capture.[1,9,10] Very recently, the relevance of electron promotion has been demonstrated by experiments of Ne atoms impact on Al surface at small incidence angles with respect to the surface plane.[11]

A mechanism called surface-assisted kinetic electron emission (sKEE) has been recently proposed in experiments of slow ions impact on metal surfaces at normal or near normal incidence.[3,12] In this mechanism, nonadiabatic excitations are allowed by a kind of localization or confinement of valence electrons by the surface potential. This model predicts that the electron emission yields decrease exponentially with the inverse of $v_\perp$, the component of the velocity of incoming ions orthogonal to the surface. The sKEE model explained the subthreshold contribution to KEE and is supported by good fits to experimental energy distribution and electron emission yields for several projectile-target systems.[3,12] In the case of slow ion impact on polycrystalline Au surfaces,[3] however, electron emission yields were reproduced by the sKEE model even far above the calculated threshold energy for the onset of electron promotion, thus raising the question of the importance of electron promotion in KEE from metal surfaces.

To examine this question, we measured energy distributions of electrons emitted from Al surfaces under the impact of 1–8 keV Kr$^+$ ions. For the Kr-Al system, KEE due to electron promotion has been extensively studied in the past.[8] In this case, Al-2p electrons are promoted in binary collisions between recoiling Al target atoms. This inner-shell excitation is evidenced in the spectra of emitted electrons in the Al-2p Auger signature and in a feature due to the decay of bulk plasmons excited by those Auger electrons traveling inside the solid (subthreshold kinetic excitation of plasmons[2]). These spectroscopic features are superimposed on a continuum background spectrum due to the cascade of electron-electron collisions, which is a characteristic of KEE.

We observe that total electron emission yields, γ_{tot}, do not show the angular behavior predicted by sKEE models. For fixed incidence angle, γ_{tot} follow an exponential behavior with $1/v$, for impact velocities above the threshold for Al-Auger excitation. The same behavior occurs for the intensity of Auger and plasmon decay electrons, extracted from the measured electron energy distributions by a very simple data analysis. Therefore, it is concluded that kinetic electron excitation in the interaction of Kr$^+$ ions with Al surfaces is dominated by electron promotion.

II. EXPERIMENTS

The measurements were performed in an ultra-high vacuum (UHV) chamber with a base pressure of
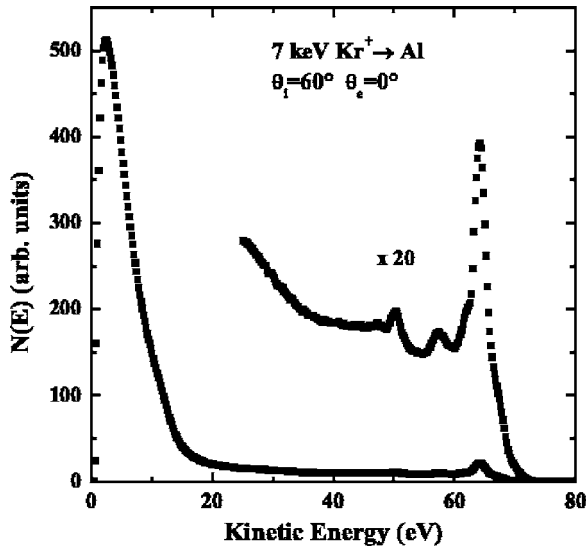
FIG. 1. Energy distribution of electrons emitted from an Al surface by 7 keV Kr$^+$ ions for the fixed experimental geometry θ_i =60°, θ_e=0°.

5×10^{-10} Torr. Kr ions were produced in a differentially pumped Atomika ion source with a discharge voltage set to $\sim$25 V to avoid significant amounts of doubly charged ions from reaching the surface with twice the energy. The ion current was of the order of 1 nA and had a Gaussian spatial distribution in both horizontal and vertical directions measured by a Faraday cup at the target position.

A polycrystalline Al sample (purity 99.999%) was sputter cleaned by 6 keV Kr ions. The sputtering was continued beyond that required to remove any detectable level of contamination by Auger spectroscopy and until the structure in the electron energy spectra became constant. Emitted electrons were collected by an electrostatic energy analyzer with a semi acceptance angle of 1.5° and operated at a constant pass energy of 50 eV. The UHV chamber is shielded with μ metal to minimize the effect of stray magnetic fields on electron trajectories.

III. RESULTS

Figure 1 shows $N(E)$, the energy distribution of electrons emitted from Al surface by 7 keV Kr$^+$ ions at an incident angle of θ_i=60° and an observation angle θ_e=0°, both measured with respect to the surface normal. The as-acquired energy spectrum is normalized to the beam current and width. The spectrum in Fig. 1 agrees with those found in the literature[2] and shows typical features of kinetic electron emission, evidenced by a broad continuum background on which discrete structures are superimposed. The broad structure visible in the 10–15 eV energy range identifies electron emission from the decay of plasmons. At higher electron energies, the spectrum show structures due to the Auger decay of Al atoms excited in the 2p shell by electron promotion either in binary asymmetric projectile-target collisions or in symmetric collisions between recoiling target atoms.[7,8] To better illustrate these features, we also amplified in Fig. 1 the relevant portion of the spectrum.
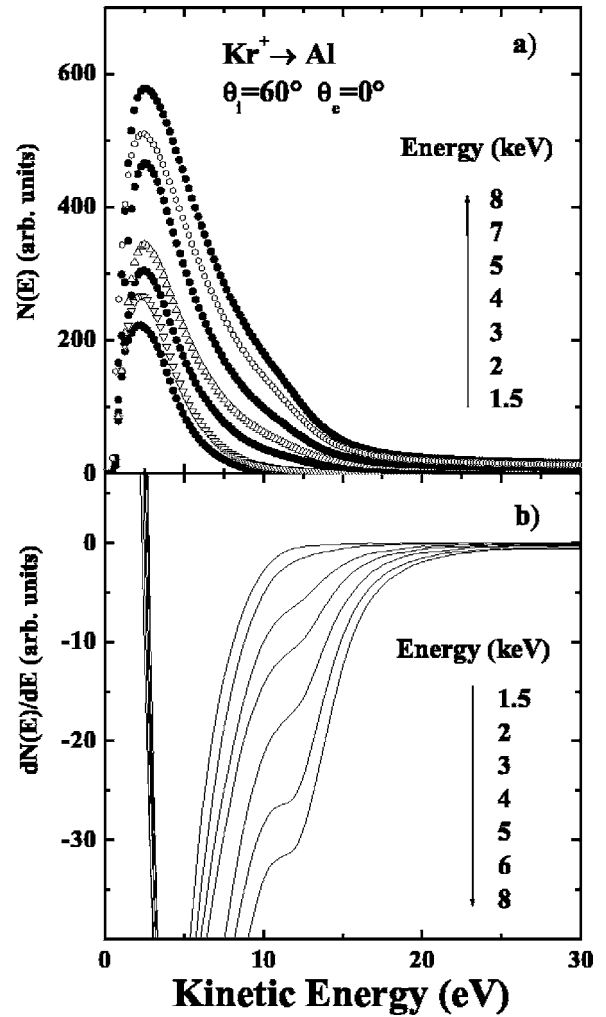
FIG. 2. Top: Energy spectra of electrons emitted from an Al surface by keV Kr$^+$ impact at different projectile energies for the fixed experimental geometry θ_i=60°, θ_e=0°. Bottom: Derivative $dN(E)/dE$ that enhances the visualization of structures due to plasmon decay.

Figure 2(a) shows the low energy portion of energy distributions of electrons emitted from the Al surface by Kr$^+$ ions as a function of incident energy for the fixed experimental geometry θ_i=60°, θ_e=0°. One can notice that the intensity of the plasmon structure increases as the incident energy increases, above a threshold projectile energy of about 1.5 keV. To easily visualize the plasmon decay, we show in Fig. 2(b) the derivative of the experimental electron energy distributions, where plasmon decay is signaled by the minima at energy $E_m = E_{pl} - \Phi$ (E_{pl} is the plasmon energy and Φ =4.3 eV is the work function for polycrystalline Al). The derivatives were obtained digitally, introducing a very slight smoothing with a Sawitsky-Golay algorithm, taking care that the smoothing did not produced artifacts or artificial broadening with respect to the unsmoothed numerical derivative. Consistent with previous studies, the minimum around 11 eV in Fig. 2(b) is assigned to electron emission from the decay of low-momentum bulk plasmons.[2,13]
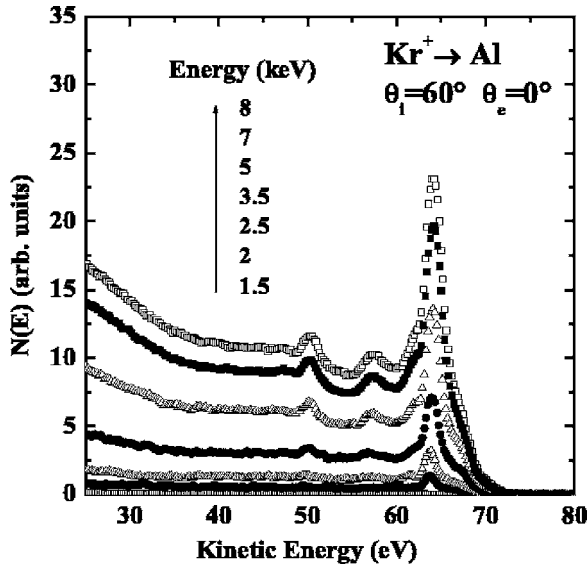
FIG. 3. Evolution of the Auger transition region in the spectra of electrons emitted from an Al surface vs the energy of Kr^+ projectiles.

Figure 3 shows the evolution of the region where Auger transitions appear with projectile energy. These features dominate the spectrum and consist of several narrow lines due to the decay of sputtered, Al-2p excited atoms, superimposed on a broad spectrum due to Al-2p Auger transitions inside the bulk and involving valence electrons.[8]

IV. DATA ANALYSIS

To obtain information about the intensity I_{BP} of electron emission from plasmon decay, one needs to devise methods to disentangle the plasmon decay structure from the background spectrum. Due to the lack of a detailed knowledge of the shape of the plasmon decay feature, several simplified methods of data analysis have been reported in the literature.[14–16] Inspite of their simplification (see e.g., Ref. 15 for a discussion), these methods allowed to depict the simple physical picture of plasmon excitation in slow ion-surface interactions. Here we apply and compare two different approaches, showing that they give consistent results.[15,16]

The first approach is based on the analysis of the experimental spectra,[15] written as $N(E)=T(E)N_0(E)$, where $N_0(E)$ is the internal energy distribution, i.e., the spectrum of electrons excited inside the solid at energy E above the vacuum level, where $T(E)$ is the surface transmission function, giving the probability that an electron of excitation energy E is transmitted through the surface barrier.

As shown in Figs. 2 and 4, our spectra are characterized by two structures: a broad continuum background and a shoulder at 9–12 eV attributed to electron emission from bulk plasmon decay. Thus, in this case, $N_0(E)=N_{0Bkg}(E)$ $+N_{0BP}(E)$, where $N_{0Bkg}(E)$ and $N_{0BP}(E)$ indicate the internal energy distribution of the two processes, respectively.
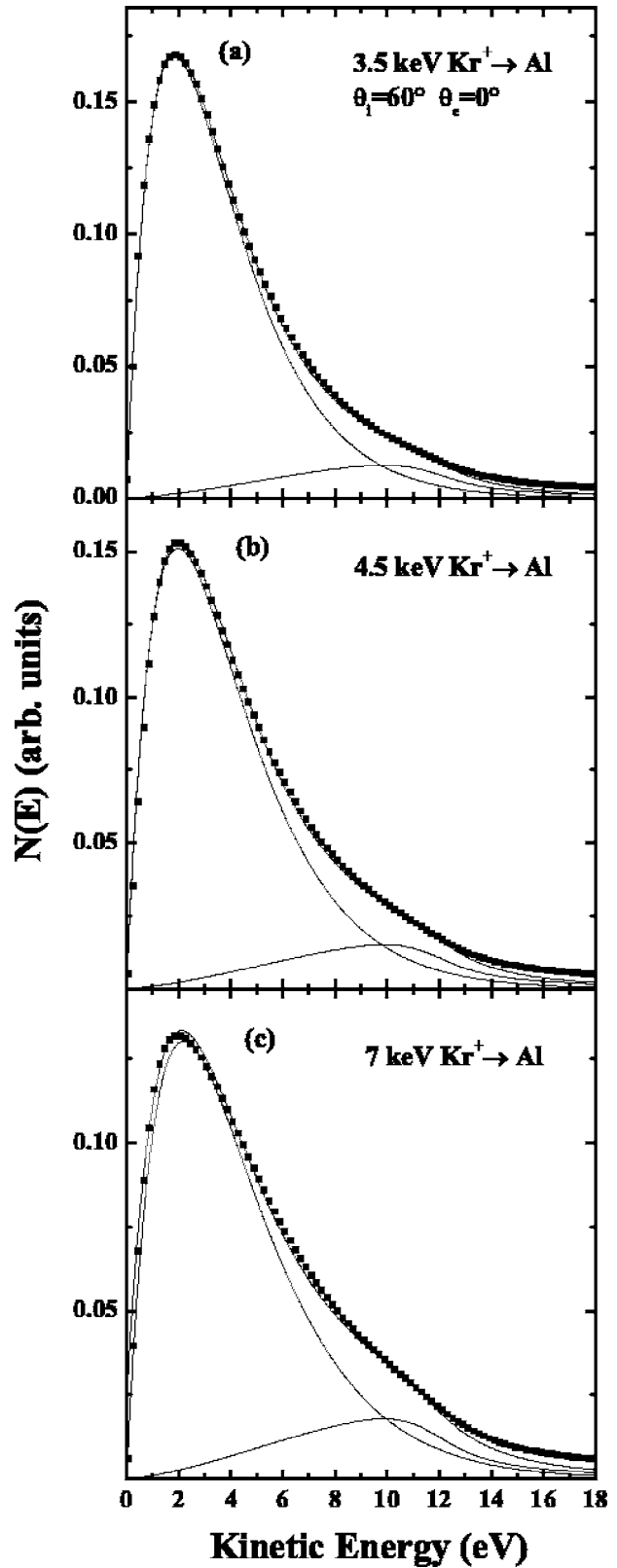
FIG. 4. Electron energy spectra from Al induced by Kr^+ ions at 3.5 keV (a), 4.5 keV (b) and 7 keV (c) reproduced by the sum of two contributions: a continuum background, $N_{Bkg}(E)$ $=T(E)N_{0Bkg}(E)$, and the plasmon decay spectrum, $N_{BP}(E)$ $=T(E)N_{0BP}(E)$. The spectra are shown normalized to a unit area.
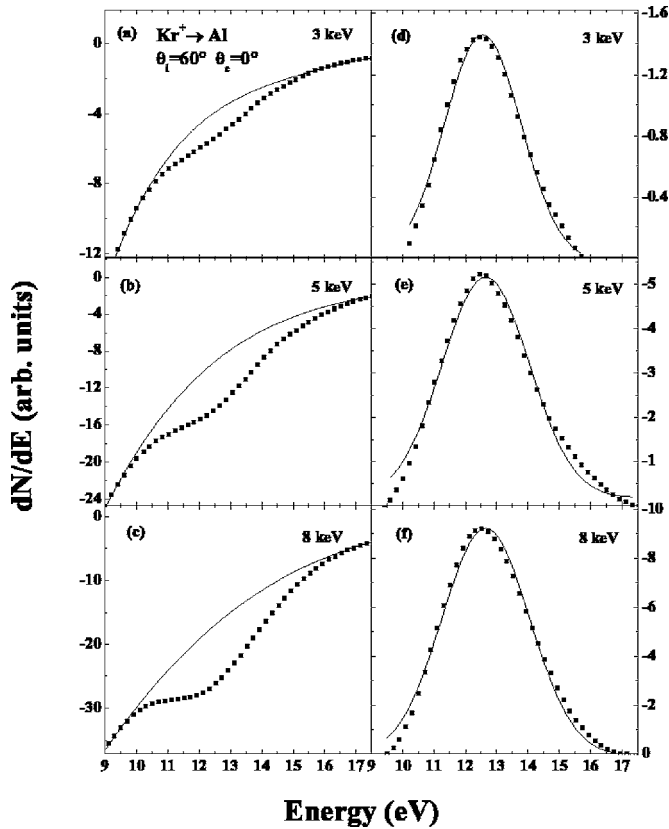
FIG. 5. (a)–(c) Examples of polynomial background subtraction from the derivative $dN(E)/dE$, for different incident energies; (d)–(f) Gaussian curve fits of the negative peaks obtained after background subtraction.

FIG. 6. The total electron emission yields γ_{tot} for $\Theta_i = 60°$ and $\Theta_i = 0°$ vs. v^{-1}, the inverse of the velocity of the projectile. I_{tot} is the area of the spectra revealed for $\Theta_i = 60°$ and $\Theta_e = 0°$. Also shown are I_{BP}, the area of the plasmon feature in the spectra, and I_{HE}, the area of the portion of the spectra due to high energy electrons. The lines through data points are used to guide the eye.

Figure 4 shows the attempt to reproduce the experimental spectra $N(E)$ of electrons emitted by 3.5 keV, 4.5 keV, and 7 keV Kr$^+$ ion impact on Al. In Fig. 4, the spectra are shown normalized so that their areas I_{tot} equal unity. For the surface transmission function $T(E)$, we chose Eq. (16) in Ref. 1. For $N_{0Bkg}(E)$, we found that an experimental function of the type $a^{-E/b}$ reproduces the background spectrum well. Finally, as in Refs. 15 and 16 for $N_{0BP}(E)$, we consider the convolution of a parabolic density of states with a Lorentzian of width chosen to be 2.5 eV for a good reproduction of the experimental spectra, also consistent with the typical lifetime width of plasmon features observed in electron energy loss experiments.

This simple analysis allows us to estimate from the experimental spectra the relative contribution due to electron emission from bulk plasmon decay as the integral of the corresponding electron energy distribution $N_{BP}(E)$ in Fig. 4, i.e., the ratio $R_{BP} = I_{BP}/I_{tot}$, where I_{BP} is the intensity of plasmon decay electrons. R_{BP} is estimated with an uncertainty of $\sim 15\%$ by varying the relative weights of the two calculated energy distributions that reproduce the experimental spectra and by using other functional forms for $N_{0Bkg}(E)$ and for $T(E)$.

The second approach to data analysis is based on the analysis of the derivative of the spectra[16] and is illustrated in Fig. 5. Panels (a)–(c) of Fig. 5 report examples of back-

ground subtraction from the derivative of the spectra. The background curve was obtained by fitting the regions on both sides of the plasmon structure with a polynomial function. Panels (d)–(f) report the negative peaks obtained after the subtraction.

We observe that at any incident energy the plasmon structure is well reproduced by just one Gaussian curve centered at the energy corresponding to the decay of bulk plasmons. These findings contrast those for He$^+$ and Ne$^+$ impact on Al and Mg surfaces,[2,15] where the bulk plasmon structure is overlapped with another structure assigned to the decay of multipole surface plasmons excited by the potential energy released when the projectile ion neutralizes at the surface, and confirm that, in the case of Kr$^+$ ions, only kinetic excitation of bulk plasmons is allowed since insufficient energy is released during neutralization at the surface.

The area I_{BP} of the plasmon feature in the experimental spectrum can be obtained from the area A_{BP} of the corresponding Gaussian in Fig. 5 by multiplying by a factor C.[16] As discussed previously,[15] the value of C is quite uncertain. Comparison with the analysis procedure described previously indicates a value of $C \sim 30$, consistent with previous estimates.[15]

V. DISCUSSION

In Fig. 6, we plot the total electron emission yield $\gamma_{tot}(60°)$ as a function of v^{-1}, the inverse of the velocity of

incoming ions. Electron yields were determined by measuring the current on the sample under positive and negative bias. Figure 6 reports also the area I_{tot} of the spectra in Figs. 1–3 which shows the same behavior. A similar result is obtained also in the case of neon projectiles, whose electron yields are known.[17,18]

For comparison, Fig. 6 reports also the yield $\gamma_{\text{tot}}(0°)$ measured in Ref. 18 at normal incidence. The fact that at any impact velocity $\gamma_{\text{tot}}(60°)$ is larger than $\gamma_{\text{tot}}(0°)$ by a factor of $\sim 2 = \cos(60°)^{-1}$ is in contrast with models of sKEE that predict that the yields decrease exponentially with $1/v_\perp$, the inverse of the component of v orthogonal to the surface. We note that a plot vs $1/v_\perp$ would separate the yields at 0 and 60° even more than is shown in Fig. 6.

On the other hand, the fact that $\gamma_{\text{tot}}(60°)$ and $\gamma_{\text{tot}}(0°)$ follow a very similar behavior with $1/v$ is consistent with models of KEE resulting from binary atomic collisions, which suggest that the excitation cross sections at low velocities decrease exponentially with $1/v$, similar to the case of ionization collisions in the gas phase, as pointed out previously.[19] Indeed, we observe that γ_{tot} approach an exponentially increasing trend with decreasing v^{-1} below the threshold for the observation of electron promotion effects (vertical line in Fig. 6) in the 35–80 eV electron energy range of our spectra. The dependence on incident ion energy of the area I_{HE} of this portion of the spectrum is nicely consistent with published yields of Al-2p Auger electron emission,[8] including the threshold behavior. This confirms that the increase of emission in the high electron energy range is dominated by Auger electron emission resulting from electron promotion during binary collisions between recoiling target atoms.[8] We observe that I_{HE} contributes to a minor fraction of I_{tot}. However, it is well known that bulk plasmons are excited by energetic electrons traveling inside the solid.[2] Indeed, we observe that electron emission from plasmon decay has the same threshold and the same growing trend as I_{HE}. This is also shown in Fig. 7(a) by the constancy of the intensity ratio $R = I_{\text{BP}}/I_{\text{HE}}$ with projectile energy. The fact that I_{BP} is about twice as large as I_{HE} indicates that energetic electrons scatter very efficiently inside the solid and produce further electronic excitation, such as the observed bulk plasmons.

Figure 7(b) shows the ratios $R_{\text{BP}} = I_{\text{BP}}/I_{\text{tot}}$ and $R_{\text{HE}} = I_{\text{HE}}/I_{\text{tot}}$ and compares them with the ratio $R_D = CA_{\text{BP}}/I_{\text{tot}}$ obtained from the analysis of the derivatives of the experimental spectra, showing thus that the two analysis methods give the same results.

We observe that above the threshold energy for electron promotion, R_{BP} and R_{HE} increase with incident ion energy approaching a constant value. The observations reported in Figs. 6 and 7 indicated that the continuum part of the spectrum is produced by the electronic collision cascade initiated by energetic electrons, excited in Auger transitions and in the decay of bulk plasmons, establishing that electron promotion is the dominant mechanism for electron emission.

The weak electron emission that occurs below the threshold energy for electron promotion can be assigned to the potential electron emission due to Auger neutralization of
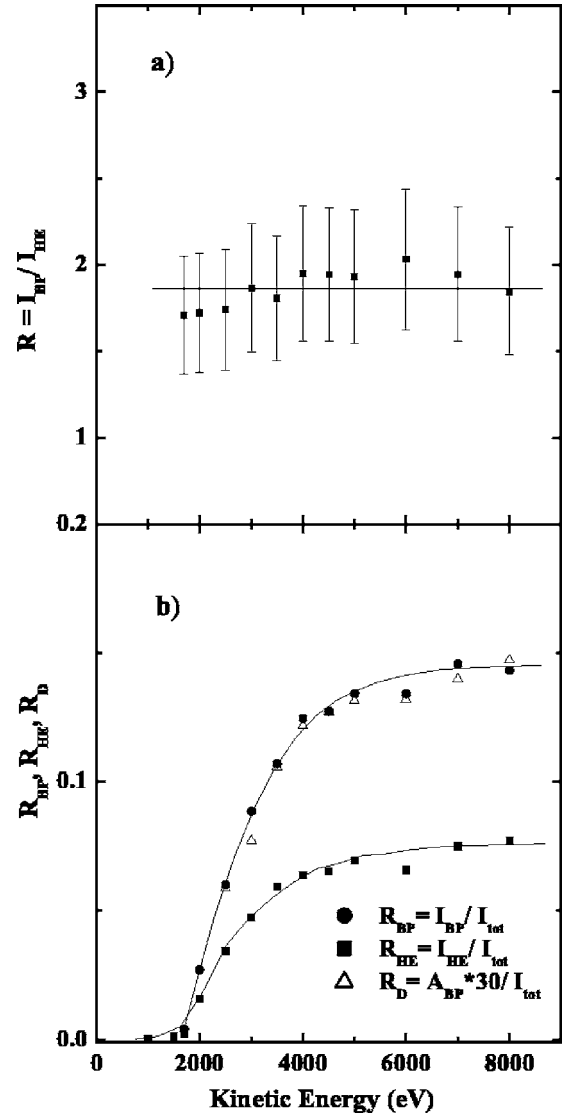
FIG. 7. Top: Ratio $R = I_{\text{BP}}/I_{\text{HE}}$ vs projectile energy. Bottom: $R_{\text{BP}} = I_{\text{BP}}/I_{\text{tot}}$, $R_{\text{HE}} = I_{\text{HE}}/I_{\text{tot}}$, and $R_D = CA_{\text{BP}}/I_{\text{tot}}$ ($C = 30$). The lines through data points are used to guide the eye.

Kr$^+$ at the surface[20] and to nonadiabatic excitation caused by the finite interaction time of the projectile with the surface[3,12] or to outer shell promotion in close collisions. At present there is insufficient information to distinguish between the different mechanisms.

VI. CONCLUSIONS

Measurements of both total electron yields and energy spectra in the interaction of slow Kr$^+$ ions with Al surfaces give deep insight into different electron emission mechanisms, showing the interplay between these processes. The comparison of the yields at 60° incidence to those at normal incidence[18] show that the total yield of electron emission does not have the dependence on $1/v_\perp$ predicted by the recently proposed sKEE model, evidencing the dominance of electron promotion in this case. Nevertheless, this result is not contradictory with the claim of the existence of the sKEE

mechanism, which explained experiments on systems for which electron promotion is not expected.[12] For the Kr-Al system, we cannot rule out the contribution to kinetic electron excitation by sKEE, below the threshold energy for electron promotion. In the case of noble gas ions, this subthreshold energy range is masked by potential energy effects, calling for further experimental investigations using projectiles of low ionization potential, such as alkali ions.

*Corresponding author. Electronic address: riccardi@fis.unical.it

[1] R. A. Baragiola, in *Low Energy Ion-Surface Interaction*, edited by J. W. Rabalais (Wiley, New York, 1994), Chap. 4.

[2] R. A. Baragiola, C. A. Dukes, and P. Riccardi, Nucl. Instrum. Methods Phys. Res. B **182**, 73 (2001).

[3] J. Lorincik, Z. Sroubek, H. Eder, F. Aumayr, and H. Winter, Phys. Rev. B **62**, 16116 (2000).

[4] S. Lederer, K. Maass, D. Blauth, H. Winter, H. P. Winter, and F. Aumayr, Phys. Rev. B **67**, 121405(R) (2003).

[5] R. A. Baragiola, E. V. Alonso, and A. Oliva Florio, Phys. Rev. B **19**, 121 (1979); H. Winter and H. P. Winter, Europhys. Lett. **62**, 739 (2003).

[6] M. Barat and W. Lichten, Phys. Rev. A **6**, 211 (1972).

[7] S. Valeri, Surf. Sci. Rep. **17**, 85 (1993).

[8] R. A. Baragiola, E. V. Alonso, and H. J. L. Raiti, Phys. Rev. A **25**, 1969 (1982); N. Mandarino, P. Zoccali, A. Oliva, M. Camarca, A. Bonanno, and F. Xu, Phys. Rev. A **48**, 2828 (1993).

[9] G. Zampieri, F. Meier, and R. Baragiola, Phys. Rev. A **29**, 116 (1984).

[10] L. Guillemot, S. Lacombe, V. N. Tuan, V. A Esaulov, E. Sanchez, Y. A. Bandurin, A. I. Dashchenko, and V. G. Drobnich, Surf. Sci. **365**, 353 (1996).

[11] Y. Matulevich, S. Lederer, and H. Winter, Phys. Rev. B **71**, 033405 (2005).

[12] J. A. Yarmoff, H. T. Than, and Z. Sroubek, Phys. Rev. B **65**, 205412 (2002); J. A. Yarmoff, H. T. Than, and Z. Sroubek, Nucl. Instrum. Methods Phys. Res. B **193**, 667 (2002).

[13] M. S. Chung and T. E. Everhart, Phys. Rev. B **15**, 4699 (1977).

[14] N. Bajales, S. Monitoro, E. C. Goldberg, R. A. Baragiola, and J. Ferrón, Surf. Sci. Lett. **579**, L97 (2005).

[15] P. Riccardi, A. Sindona, P. Barone, A. Bonanno, A. Oliva, and R. A. Baragiola, Nucl. Instrum. Methods Phys. Res. B **212**, 339 (2003).

[16] N. Stolterfoht, D. Niemann, V. Hoffmann, M. Rosler, and R. A. Baragiola, Phys. Rev. A **61**, 052902 (2000).

[17] K. Wittmack, Nucl. Instrum. Methods Phys. Res. B **115**, 288 (1996).

[18] E. V. Alonso, R. A. Baragiola, J. Ferrón, M. M. Jakas, and A. Oliva-Florio, Phys. Rev. B **22**, 80 (1980).

[19] R. A. Baragiola, Nucl. Instrum. Methods Phys. Res. B **88**, 33 (1994).

[20] H. D. Hagstrum, Y. Takeishi, and D. D. Pretzer, Phys. Rev. **139**, 526 (1965).